Concrete Girders Externally Prestressed With Composite Plates

Mohan S. Char
Graduate Research Assistant
Department of Civil Engineering
and Engineering Mechanics
University of Arizona
Tucson, Arizona

Hamid Saadatmanesh Ph.D., P.E.
Associate Professor of Civil Engineering and Engineering Mechanics
University of Arizona
Tucson, Arizona

Mohammad R. Ehsani Ph.D., P.E.
Associate Professor of Civil Engineering and Engineering Mechanics
University of Arizona
Tucson, Arizona

A parametric study of the flexural strength of concrete girders externally prestressed with epoxy bonded fiber reinforced plastic (FRP) plates is presented. The girders are externally prestressed with FRP plates epoxy bonded to the tension face of the girders, while the girders are held cambered by means of upward jacking forces. The variables considered in the study are the type of FRP plate, the area of the plate, and concrete compressive strength. A design example is also presented to show the effectiveness of this strengthening technique for upgrading the load carrying capacity of a typical concrete bridge originally designed for H15 loading to that of HS20 loading.

Many of the bridges in the United States are in need of replacement and/or rehabilitation. A large number of these bridges were originally designed to carry smaller vehicles, lighter loads and lower traffic volume than are common today. This has left most of these bridges with inadequate load carrying capacity for today's traffic. Therefore, in addition to maintenance, strengthening is also necessary in older bridges to bring their load carrying capacities up to current standards.

In many cases rehabilitation takes precedence over replacement for its cost effectiveness. The more costly bridge replacement can be avoided by rehabilitating the bridge early, before deterioration reaches an advanced stage. In fact, the Federal Highway Administration recommends that before replacing a bridge, rehabilitation be given primary consideration.

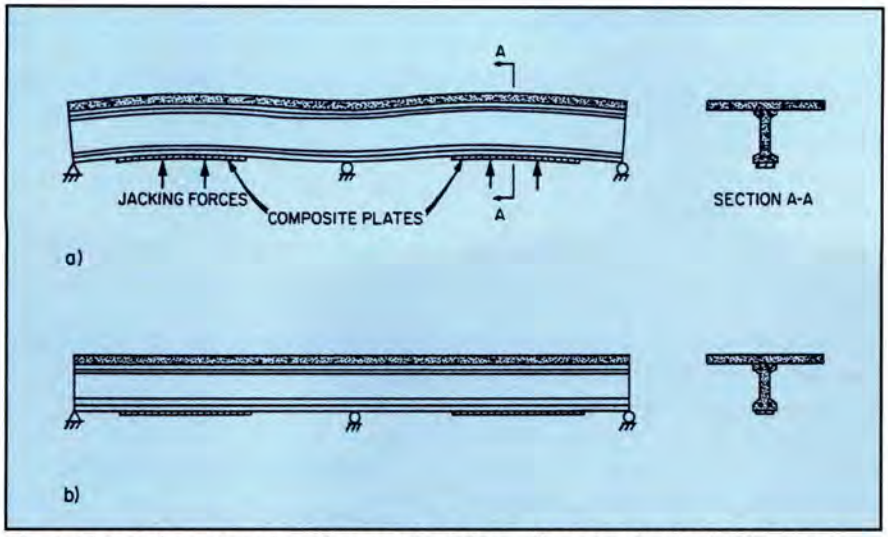

Fig. 1. External prestressing of concrete girders with epoxy bonded FRP plates — (a) camber by jacking; (b) jacks are removed when epoxy has cured.

Several different methods can be used to increase the live load capacity of existing bridges: external post-tensioning, epoxy bonding of steel plates to the tension flange, and epoxy bonding of plastic plates to the tension flange.

There are a number of existing bridges in which external post-tensioning has been used successfully to increase the strength of girders. In this technique, high strength steel cables are anchored to steel or concrete girders and tensioned to improve elastic response, ultimate capacity and fracture behavior.[1,2,3] This method poses several problems at the time of construction and during service life, including the anchoring of post-tensioning strands, maintenance of lateral stability of the girders during post-tensioning and protection of strands against corrosion.

Epoxy bonded steel plates have also been used to increase the strength of girders in existing bridges and buildings. This technique involves attaching a steel plate to the tension flange, using epoxy, to increase the strength as well as the stiffness of the structure. Even though this technique has met with success in many countries, its major problem has been corrosion of the steel plate, which adversely affects the bond strength at the epoxy-concrete interface.

An effective method for eliminating the corrosion problem in the plate bonding technique is to replace the steel plate with corrosion-proof fiber reinforced plastic (FRP) plates. Other advantages of FRP plates include high strength and light weight. In the plate bonding technique, it is advantageous to externally prestress the girder at the time of strengthening.

External prestressing is accomplished by cambering the girder with hydraulic jacks while in loose contact with an epoxy coated FRP plate, as shown in Fig. 1(a). When the epoxy is cured, the jacks are removed [see Fig. 1(b)]. The FRP plate, placed in tension, will prevent a complete elastic return of the girder. This results in initial compression and tensile stresses in the bottom and top flanges that oppose the stresses induced by service loads. Additionally, this technique of prestressing does not require the use of anchorages, so construction is simplified.

PREVIOUS STUDIES

Several researchers have studied the behavior of concrete girders strengthened with epoxy bonded steel plates.

The work of MacDonald and Calder involved testing a series of 6 x 10 in. (150 x 250 mm) rectangular beams, with lengths varying from 11.5 to 16 ft (3.5 to 4.9 m), that were strengthened with epoxy bonded steel plates.[4] They reported significant improvements in the ultimate strength of the strengthened beams. Several beams that had been exposed to the outside environment showed a smaller ultimate strength. This reduction in the ultimate strength was attributed to corrosion at the interface of steel and epoxy.

Another study by Jones et al. reported the behavior of plain and reinforced concrete beams strengthened with steel plates bonded by epoxy to the tension face of the beams.[5] They used two different types of adhesive and two grades of steel plate. The effects of adhesive thickness, plate lapping, multiple plates, and of precracking prior to bonding were investigated. They concluded that external prestressing with steel plates resulted in enhancement of elastic range, reduction in tensile stresses, increase in strength and stiffness, and improvements in ductility at flexural failure.

Saadatmanesh and Ehsani tested several concrete beams externally reinforced with glass fiber reinforced plastic (GFRP) plates.[6] They first conducted a series of tests on small-scale beams to examine their behavior and to select a suitable epoxy for this strengthening technique. They tested five beams, each having a cross section of 3.5 x 6 in. (90 x 150 mm) and a length of 66 in. (1.67 m). The beams had one No. 3 Grade 60 bar for tension reinforcement and $^{3}/_{16}$ in. (5 mm) diameter wires placed at 3 in. (75 mm) for shear reinforcement.

The GFRP plates were $^{1}/_{4}$ x 3 in. (6 x 75 mm) in cross section and were attached to only four of the five beams tested. The fifth beam was the control beam. They also used different types of epoxy on each of these four beams. It was concluded that the behavior of these beams was very similar to that of their counterparts strengthened with steel plates, with the added advantage of resistance to corrosion. They attributed the success of this technique to the use of a suitable epoxy. It was suggested that the epoxy should have sufficient stiffness, strength and toughness like that of rubber-toughened epoxies.

On completion of small-scale tests, they carried out another series of tests on five rectangular beams and one T-beam.[7] The rectangular beams were 18 x 8 in. (455 x 205 mm) in cross section. The flange width and thickness of the T-beam were 24 and 3 in. (610 and 75 mm), respectively. The overall height was 18 in. (455 mm) and the thickness of the web was 8 in. (205 mm). The overall length of each beam

was 16 ft (4.88 m) and the beams were supported on a clear span of 15 ft (4.57 m) during the test.

Three different reinforcement ratios were used for the beams. The GFRP plates were 6 x 1/4 in. (152 x 6 mm) in cross section and 14 ft (4.26 m) long. These plates were attached to the tension flanges of the beams. They reported a significant increase in the flexural strength. The increase in the flexural strength was much greater in beams that had lower steel reinforcement ratios. They also found that plating contributed, in part, to reduction in ductility. Reduction in crack sizes was observed at all load levels.

Ritchie et al. recently investigated the external reinforcement of concrete beams using fiber reinforced plastics.[8] Sixteen beams were tested in their study. They utilized three different types of fiber composite plates — glass, carbon, and aramid. Two of the beams tested were control beams. Glass fiber reinforced plates were used on eight beams, carbon on two beams, aramid on one beam, and steel plates on the remaining two. The reinforcing steel yielded in most of the beams before failure. Shear failure occurred in the beam strengthened by aramid plates.

It was reported that a significant increase in the ultimate moment capacity of the beams was observed. Their proposed theoretical model was in reasonable agreement with their experimental work. They suggested the use of rubber-toughened epoxy for this structural system. It was also recommended that, while choosing epoxies, due consideration be given to their strength, creep, fatigue, environmental stability and compatibility with materials being bonded.

Strengthening of concrete beams with carbon plates has been in use for some time in Switzerland. There are several field application cases for buildings and bridges, as summarized by Meier et al.[9] In addition, Triantafillou et al. have demonstrated the effectiveness of strengthening beams with prestressed carbon sheets.[10] Five 47 in. (1.2 m) long beams were tested. Carbon sheets were stretched and epoxied to the tension flanges of the beams. All beams exhibited superior strength and stiffness improvements.

FIBER REINFORCED PLASTICS

Fiber Reinforced Plastics (FRP) are becoming increasingly popular as structural components. FRPs have several distinct advantages over steel. Their high strength to weight ratio, corrosion resistance and light weight make them attractive materials for the solution of many civil engineering problems where conventional materials do not perform well.

FRPs are made of small fibers placed in a resin matrix. The fibers provide the composites with their unique structural properties. The resin functions primarily as a bonding agent for the fibers. FRPs are generally anisotropic. Their mechanical properties vary depending on the amount and the orientation of fibers in the direction of measurement. Additives can be used in composites to improve their fire retardancy and resistance to ultraviolet rays.

The most common type of fiber used in FRPs is glass. Glass fiber reinforced plastics (GFRPs) are the least expensive and have satisfactory structural properties. The tensile strength of unidirectional GFRPs is in excess of 100 ksi (689 MPa); however, they have a relatively low modulus of elasticity, i.e., in the order of 7000 ksi (48 GPa). The FRPs behave linearly elastic to failure. The strength and stiffness of FRPs can be significantly increased by using more advanced fibers, such as carbon. Carbon fiber reinforced plastics (CFRPs) can reach ultimate strengths in excess of 350 ksi (2400 MPa) with a modulus of elasticity of 23,000 ksi (160 GPa) or more.

The fatigue and creep behaviors of composites are also very good. Unidirectional glass reinforced composites do not fatigue when stressed below 50 percent of their tensile strength. Most of the commercially available fibers, such as glass, carbon, and boron, do not creep.[11]

OBJECTIVES

1. Present analytical models for flexural analysis of concrete girders externally prestressed with composite plates.

2. Examine the effects of design variables, such as concrete compressive strength, type of composite plate and stiffness and area of plate, on the static strength of the prestressed girders.

3. Demonstrate, through a design example, the effectiveness of this strengthening technique for upgrading the load carrying capacity of an existing bridge originally designed for H15 truck loading to that of HS20 truck loading.

ANALYTICAL STUDY

Analytical models are presented to calculate moment and curvature for concrete girders externally prestressed with FRP plates throughout the entire range of loading up to failure. The following assumptions are made in the analysis:

- Linear strain distribution across full depth of beam
- Small deformation
- No creep and shrinkage deformations
- Complete composite action between FRP plate and concrete beam, i.e., no slip
- No shear deformations

These assumptions are the same as those made in classical theories of reinforced concrete members subjected to flexure.

The stress-strain curve is idealized by Hognestad's parabola with a maximum concrete strain of 0.003.[12] The stress-strain relation for Grade 60 steel used in the study is assumed to be elastic-perfectly plastic with a yield stress of 60 ksi (411 MPa). A linear stress-strain relation up to failure is assumed for FRP plates. The stress-strain curves for Grade 60 reinforcing bar, and GFRP and CFRP plates are shown in Fig. 2. The strain compatibility method is used to calculate the forces and deformations across the depth of the cross section.

The basic steps taken in this process are as follows. Given the value of concrete strain in the extreme compression fiber, the depth of the neutral axis, c, is obtained from equilibrium of forces across the depth of the cross section. After the location of the neutral axis is determined, the strains in the concrete, steel reinforcing bar and FRP plate can be calculated using the

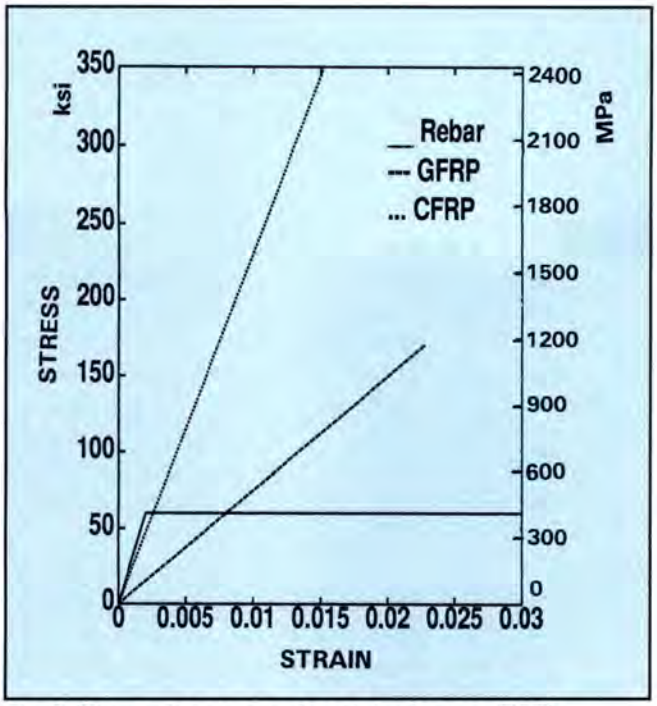

Fig. 2. Stress-strain curves for reinforcing bar, CFRP, and GFRP.

linear strain diagram. The stresses in the concrete, steel reinforcing bar and plastic plate are then obtained from their respective stress-strain curves.

The internal forces are calculated by multiplying the stresses by their corresponding areas. The moment capacity of the section is found by summing the moments of all internal forces about the neutral axis. The corresponding curvature is calculated by dividing the strain in the extreme compression fiber by the distance to the neutral axis. A computer program was developed to carry out the above computations.

The experimental results of a concrete beam externally prestressed with GFRP plate were used to verify the computer program. The beam tested had an 8 x 18 in. (205 x 455 mm) rectangular cross section and was 15 ft (4.57 m) long. It was reinforced with two No. 4 Grade 60 tension bars and two No. 4 compression bars. The concrete compressive strength was 5040 psi (35 MPa).

The beam was cambered before a 1/4 x 6 in. (6 x 150 mm) GFRP plate was bonded to the tension face along the full length of the beam. The dead load of the beam was small because it did not have a deck as an actual beam in a bridge would have. As a result, only a small cambering force could be applied to prevent severe cracking of the top face of the beam. Fig. 3(a) shows with a solid line the measured load vs. deflection to failure. The calculated load vs. deflection is shown with the dashed line. As can be seen from the figure, the measured and calculated values correlated well throughout the entire range of loading.

Fig. 3(b) shows the measured and calculated load vs. strain in tension steel reinforcing bars. The two curves correlated well up to a load of about 18 kips (80 kN). Beyond this point the measured strains were smaller than the calculated values. This can be attributed to cracking of the concrete in the vicinity of the strain gauge and possible damage to the gauge.

The measured and predicted load vs. strain in the GFRP plate are shown in Fig. 3(c). In the initial stages of loading, the measured strains in the plate were slightly less than the predicted values. As loading increased, so did the difference between the two strains. This small difference can be attributed to a slight slip in the epoxy at the interface of the plate and concrete. Fig. 3(d) shows the load vs. strain in the extreme compression fiber of concrete. Initially, the agreement between the measured and calculated values was very good. At higher levels of loading, the difference between the two curves increased.

Fig. 3(e) shows the beam at failure, which occurred as a result of shear failure of the concrete layer between the plate and longitudinal steel reinforcing bars. No delamination and/or bond failure was observed at the interface of the plate and concrete, indicating satisfactory performance of the epoxy. It is noted that the flexural strength of this beam increased by a factor of four above that for the same beam with no plate.

A comparison of the analytical and experimental results indicates that the behavior of externally prestressed concrete girders can be predicted with reasonable accuracy. The data shown in Fig. 3 indicate that the measured strains compare favorably with the predicted values. As expected with higher loads, some differences exist between these values. This is because the strains are measured over a very short gauge length and are, therefore, significantly influenced by the formation of cracks in their vicinity.

Nonetheless, there is close agreement in the trends of the measured and calculated values. Furthermore, there is close agreement between the measured and calculated load vs. deflection behavior. This is because the deflections are calculated by integrating the curvature over the entire length of the beam. Hence, they are not significantly affected by the small variations in local strain measurements shown in Figs. 3(b) through 3(d).

PARAMETRIC STUDY

In the parametric study, the effects of the initial camber and type and area of the composite plate on the moment-curvature relationship of the girder were examined. Two different types of composite plate — glass fiber reinforced plastic (GFRP) and carbon fiber reinforced plastic (CFRP) — are used in the parametric study. The ultimate strength and the modulus of elasticity of the plates are 170 ksi (1166 MPa) and 7500 ksi (51 GPa) for the GFRP plate, and 350 ksi (2400 MPa) and 23,000 ksi (158 GPa) for the CFRP plate.

The stress-strain curves of GFRP and CFRP plates are shown in Fig. 2. To show the effect of plate size on the strength and ductility of upgraded girders, two different plate areas are used for each type of composite plate: A_{pl} = 4 sq in. (25.8 cm^2); and A_{pl} = 8 sq in. (51.6 cm^2), where A_{pl} is the cross-sectional area of the composite plate. The concrete compressive strength for the girder is 6000 psi (41 MPa).

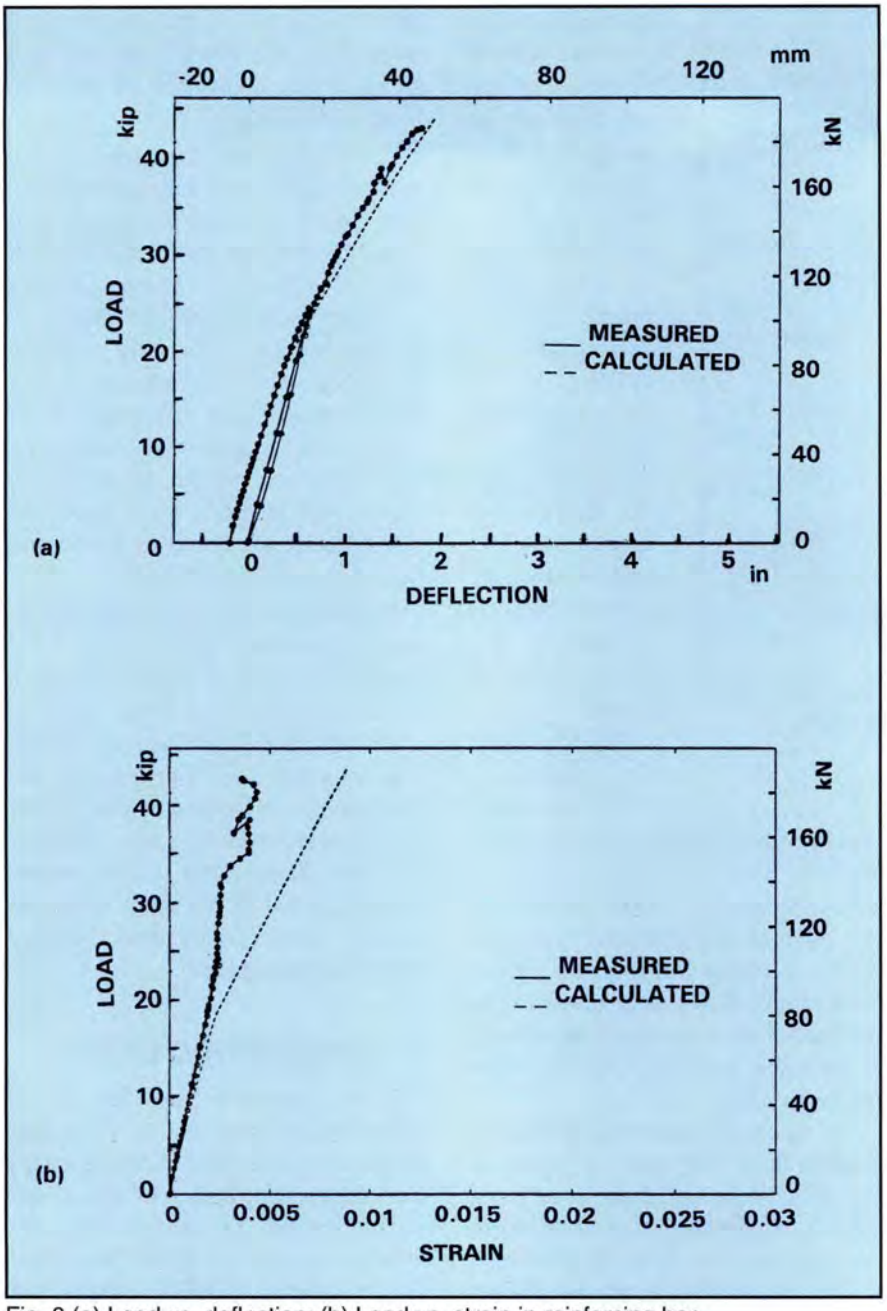

Fig. 3.(a) Load vs. deflection; (b) Load vs. strain in reinforcing bar.

The girder used in the parametric study has the following cross-sectional properties: overall height of 54 in. (1370 mm); 83 x 8 in. (2110 x 205 mm) flange; and 24 x 46 in. (610 x 1170 mm) web. The areas of tension and compression reinforcement in the girder are 9 and 6 sq in. (58 and 39 cm^2), respectively.

Table 1. Parameters used in the analysis.

Beam	Plate type	Camber	A_{pl} (in.^{2})	σ_{pl} (ksi)	E_{pl} (x 10^3 ksi)
G04	Glass	0	4.0	170	7.5
GC4	Glass	C	4.0	170	7.5
C04	Carbon	0	4.0	350	23.0
CC4	Carbon	C	4.0	350	23.0
G08	Glass	0	8.0	170	7.5
GC8	Glass	C	8.0	170	7.5
C08	Carbon	0	8.0	350	23.0
CC8	Carbon	C	8.0	350	23.0

Table 1 shows a summary of the variables used in the study. Each retrofitted beam is designated with three characters; the first character defines the type of composite plate used, i.e., G for glass and C for carbon. The second character indicates whether the beam is cambered or not, i.e., C designates camber and 0 indicates no camber, meaning that the plate is bonded to the girder in its original position without applying the jacking forces. The third character indicates the area of plate in sq in. units. For ease of comparison, the tensile strength of the plate (σ_{pl}) and its modulus of elasticity (E_{pl}) are also listed in the table.

In order to show the effectiveness of this strengthening technique, the applied moment vs. curvature and the applied moment vs. stress in the concrete, steel reinforcing bar and composite plate are discussed for the cross section shown in Fig. 4, before and after strengthening. The moment values shown on the plots include both dead load and live load moments.

In the figures to follow, each curve belonging to an upgraded beam is designated with three characters, as discussed previously. The curves with no designation belong to the girder before strengthening, i.e., the control beam.

Fig. 5(a) shows the moment vs. curvature relationship for the girder strengthened with a GFRP plate with no induced camber. The moment vs. curvature for the girder before strengthening is shown with a solid line. By comparing the moment-curvature relationships before and after strengthening, it can be seen that bonding the GFRP plate to the tension face results in a significant increase in the moment carrying capacity of the girder. This is due to the additional moment couple created by the tensile force in the GFRP plate and an equal compressive force in the deck.

Increasing the area of the plate from 4 to 8 sq in. (25.8 to 51.6 cm^2) further increased the moment carrying capacity of the section. The failure in the upgraded beams was reached as a result of rupture of the plate.

Fig. 5(b) shows the moment vs. stress in the top extreme fibers of concrete. In the control beam, the failure occurred by crushing of the concrete.

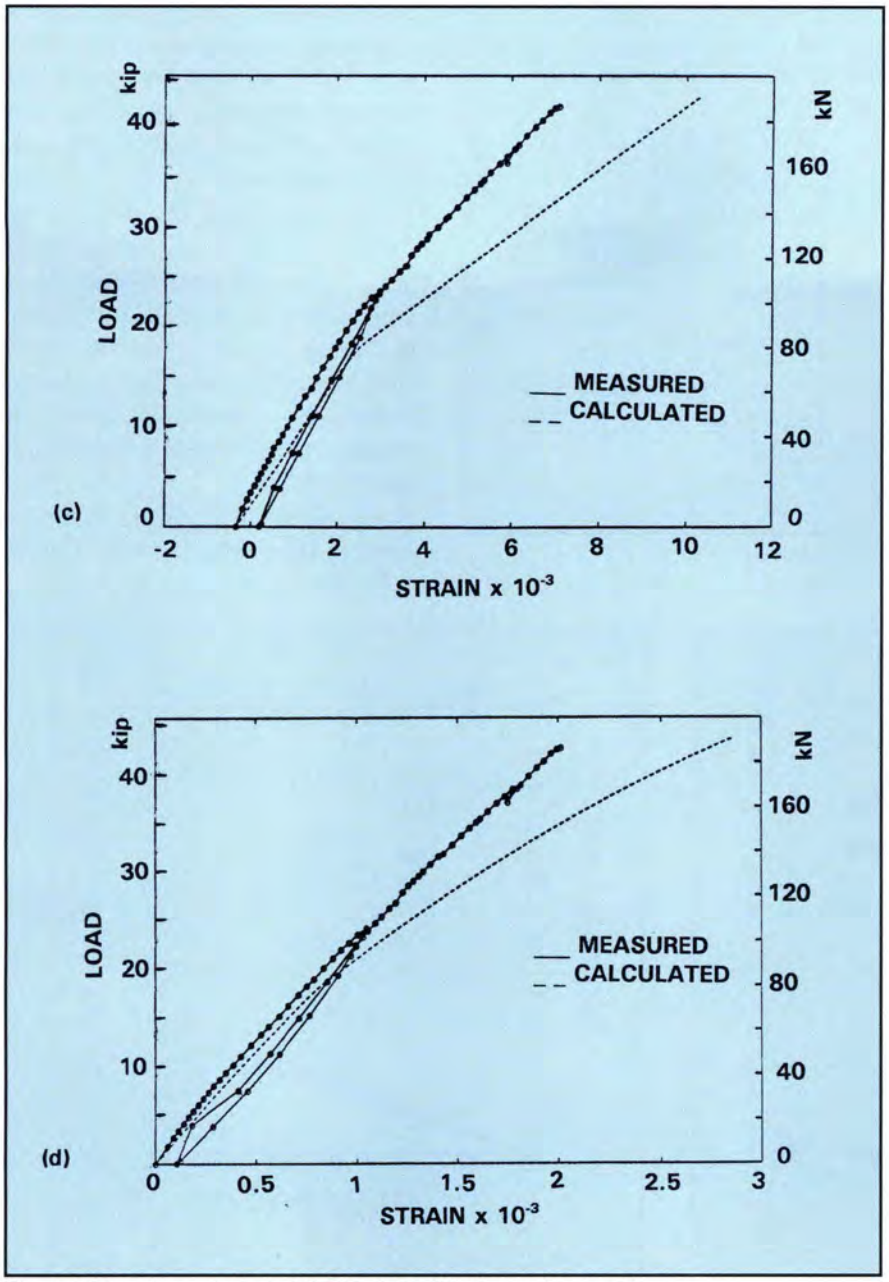

Fig. 3.(c) Load vs. strain in GFRP plate; (d) Concrete at midspan.

Fig. 3(e). Beam at failure.

The steel bars yield at a moment of 2273 kip-ft (3092 kN-m), resulting in a more rapid increase in concrete stress. The nonlinearity in the curves is due to the parabolic form of the Hognestad's stress-strain curve used in the analysis. After the tension bars yielded in the control beam, there was little increase in the moment. The strain in the concrete, however, continued to increase until it reached its crushing strain when the beam failed.

For a given moment, the beam with the 8 sq in. (51.6 cm^2) plate exhibits lower concrete stress than the beam with the 4 sq in. (25.8 cm^2) plate. The plate failed in tension before the concrete stress could reach its compressive strength value in both cases. The fracture of the plate in Specimen G08, however, was very close to the point when the concrete was reaching its compressive strength.

Fig. 5(c) contains the moment vs. stress in the reinforcing bars. In all three cases the reinforcing bars have yielded before actual failure of the beams. For a given moment, the reinforcing bar stress in the strengthened beams is slightly lower than that of the control beam, i.e., the reinforcing bars in the strengthened beams show delayed yielding.

Fig. 5(d) shows the moment vs. stress in the composite plate. The plate has reached its tensile strength value of 170 ksi (1166 MPa) in both beams. After the yielding of reinforcing bars, the tensile force created by the additional moment is carried entirely by the plate, resulting in the increased moment capacity.

Fig. 6(a) shows the moment vs. curvature for the girder externally prestressed with a GFRP plate bonded to the tension face while the girder was held cambered. The upward jacking forces were calculated to result in stresses on the top extreme fibers of the concrete equal to the modulus of rupture. In other words, jacking forces resulted in a negative moment equal to the dead load moment plus the cracking moment.

External prestressing induced a negative moment in the girder. This negative moment resulted in initial stresses in the girder as shown in Figs. 6(b) through 6(d). These initial stresses op-

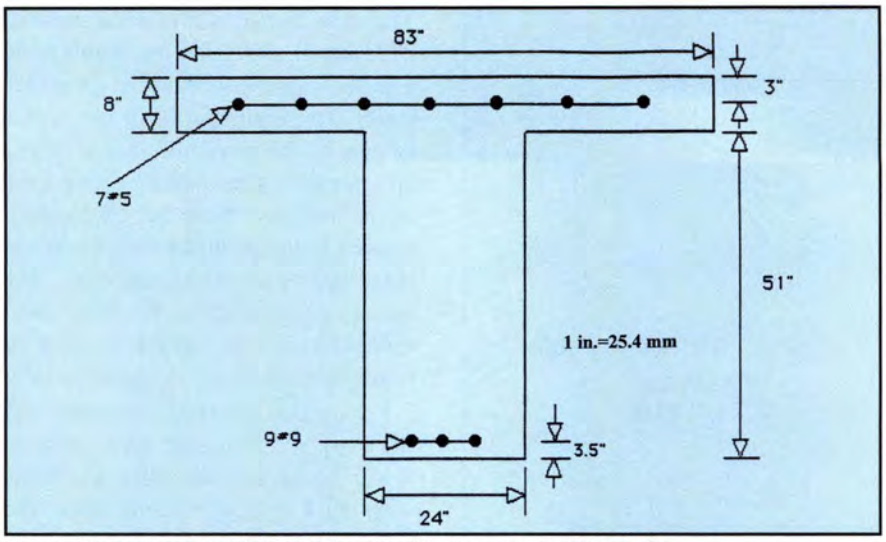

Fig. 4. Cross section of the girder used in the parametric study.

pose stresses induced by gravity loads. Cambering did not change the moment capacity of the beam from that of the previous case under no camber. The failure in the beam resulted from fracture of the plate.

Fig. 6(b) shows the moment vs. stress in the top extreme fibers of the beam. The cambering resulted in an initial tensile stress of 580 psi (4 MPa) in the top extreme fiber. The corresponding initial compressive stresses in the bottom extreme fibers will delay cracking of the beams under applied gravity loads.

Fig. 6(c) shows the moment vs. stress in the reinforcing bars. The ex-

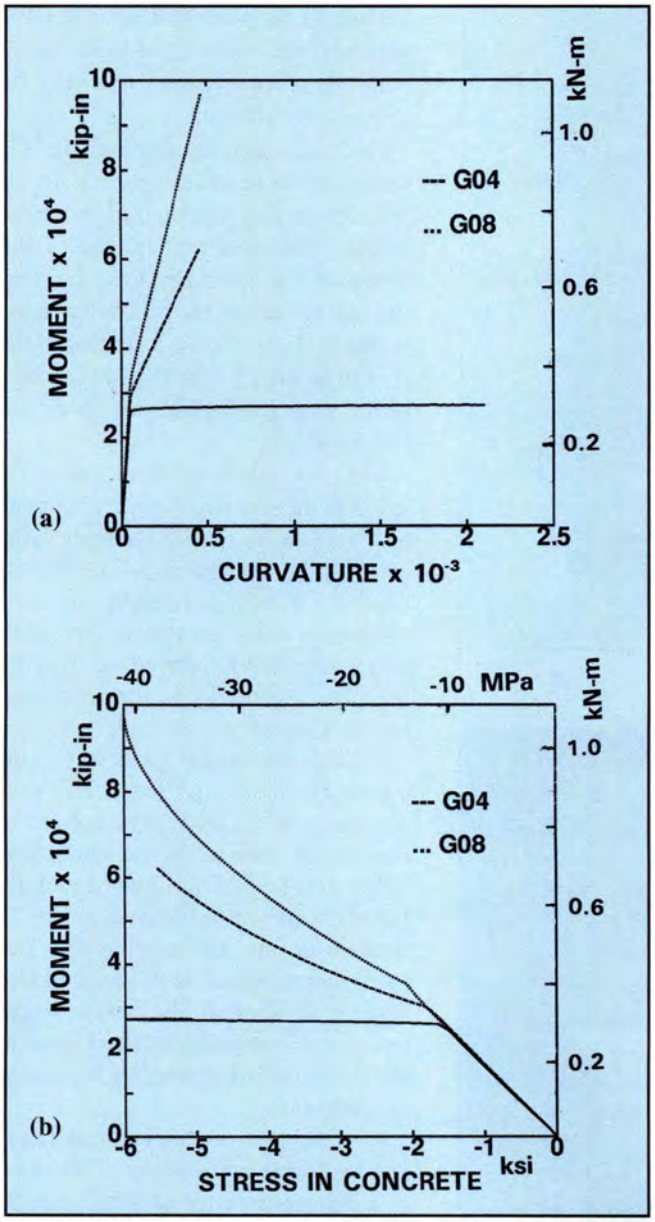

Fig. 5. (a) Moment vs. curvature; (b) Moment vs. stress in concrete midspan.

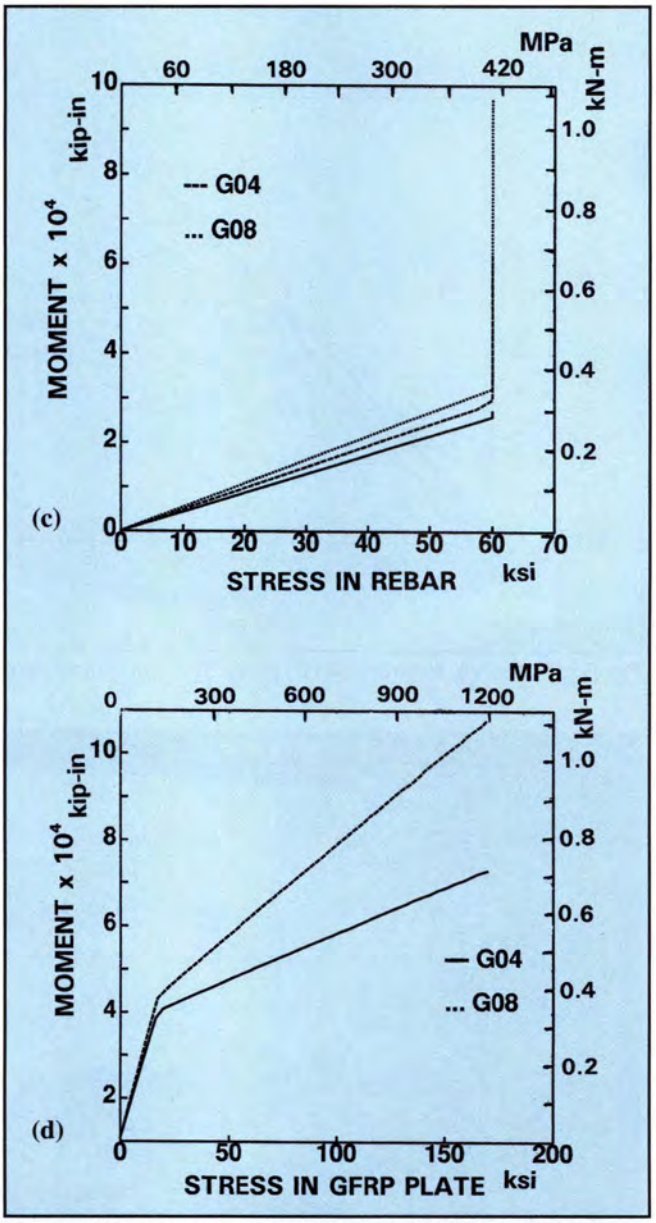

Fig. 5. (c) Moment vs. stress in reinforcing bar; (d) Moment vs. stress in GFRP plate.

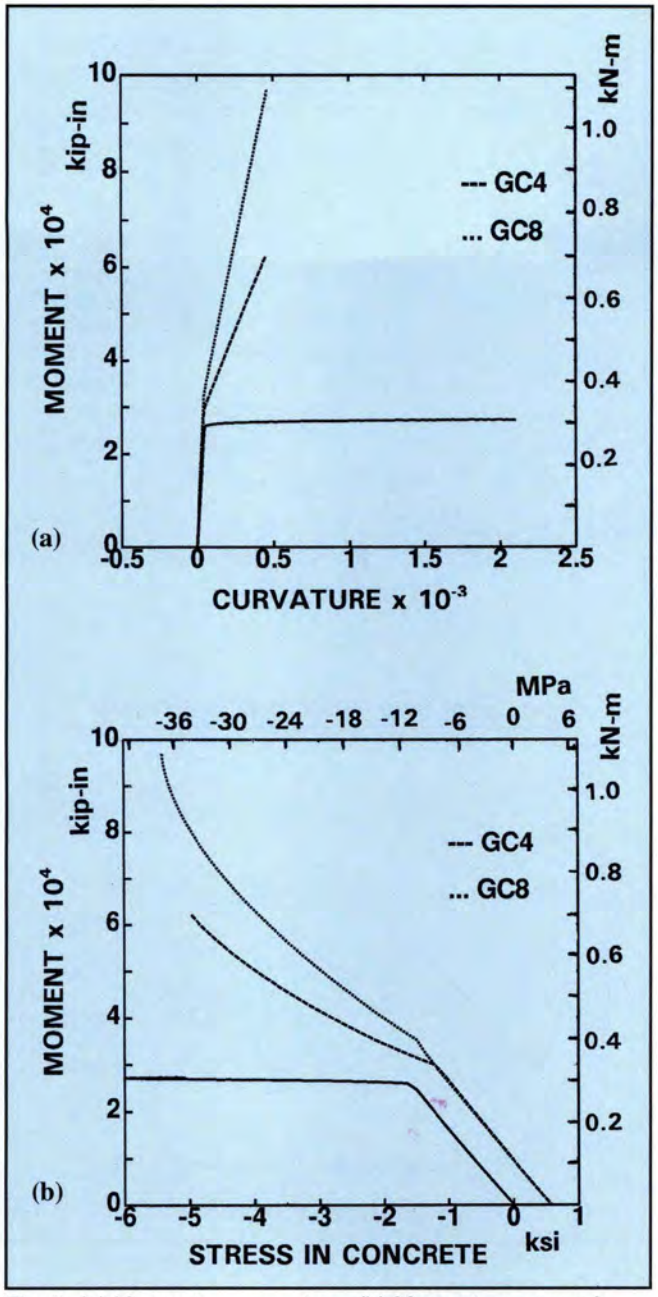

Fig. 6. (a) Moment vs. curvature; (b) Moment vs. stress in concrete.

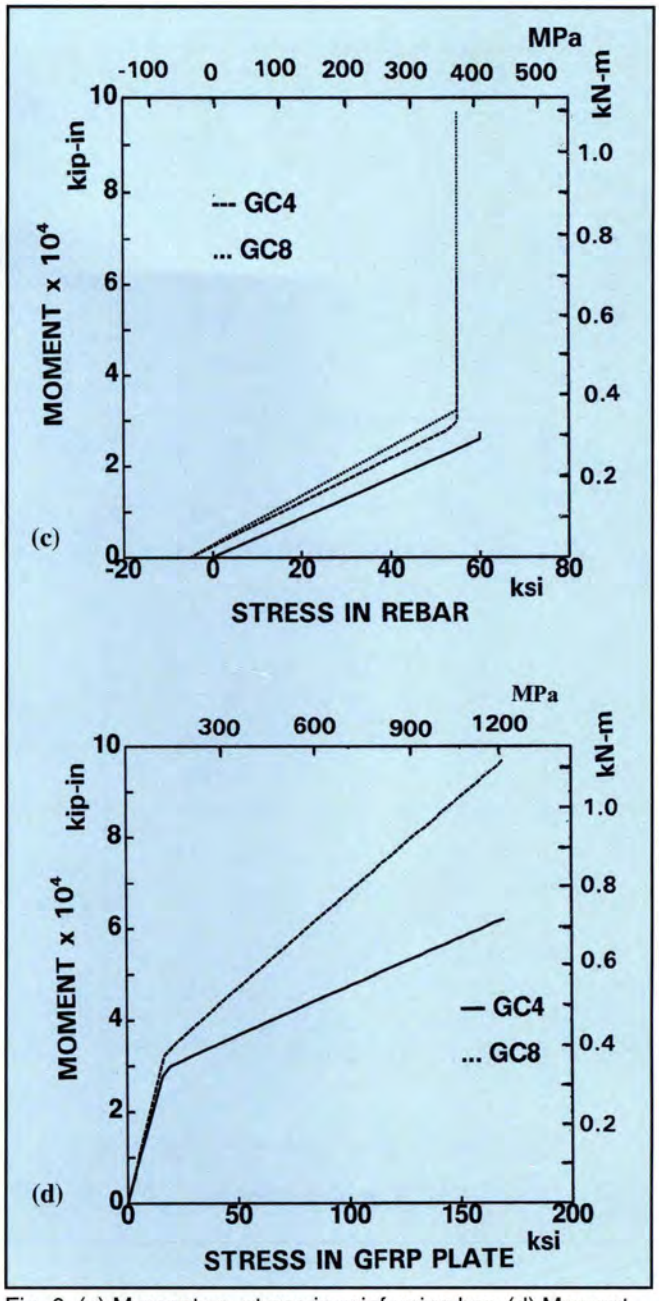

Fig. 6. (c) Moment vs. stress in reinforcing bar; (d) Moment vs. stress in GFRP plate.

ternal prestressing resulted in initial compressive stresses of about 4 ksi (27.6 MPa) in the bars. This initial stress acts in the opposite direction of the stresses induced by gravity loads and, therefore, will enlarge the elastic range of the structure; in other words, it will delay yielding of the bars.

Fig. 6(d) shows the moment vs. stress in the GFRP plate throughout the entire range of loading up to the rupture of the plate. The behavior is similar to that of the beam with no camber. The moment at fracture of the plate is slightly less than that in the beam with no camber. This is because part of the tensile strength is consumed for prestressing. Higher strength plates would be needed to achieve the same moment capacity.

Fig. 7(a) depicts the moment vs. curvature relationship of the girder strengthened with carbon fiber reinforced plastic (CFRP). The higher tensile strength of the CFRP plate resulted in a significantly greater increase in the moment capacities compared to that for the GFRP plate. The greater stiffness of the CFRP plate, however, reduced the curvature at failure of the beam compared to the beam strengthened with the GFRP plate. This reduces the overall ductility of the beam.

The moment vs. stress in the compression flange of the concrete is shown in Fig. 7(b). The beam strengthened with a plate of area 8 sq in. (51.6 cm^2) reached concrete compressive strength value at failure. In other words, the failure in the beam was reached as a result of crushing of the concrete, not rupture of the plate. The strengthened beams also exhibit significantly higher moment capacities because of the additional internal moment generated by the plate.

Fig. 7(c) shows moment vs. stress in the reinforcing bars. The reinforcing

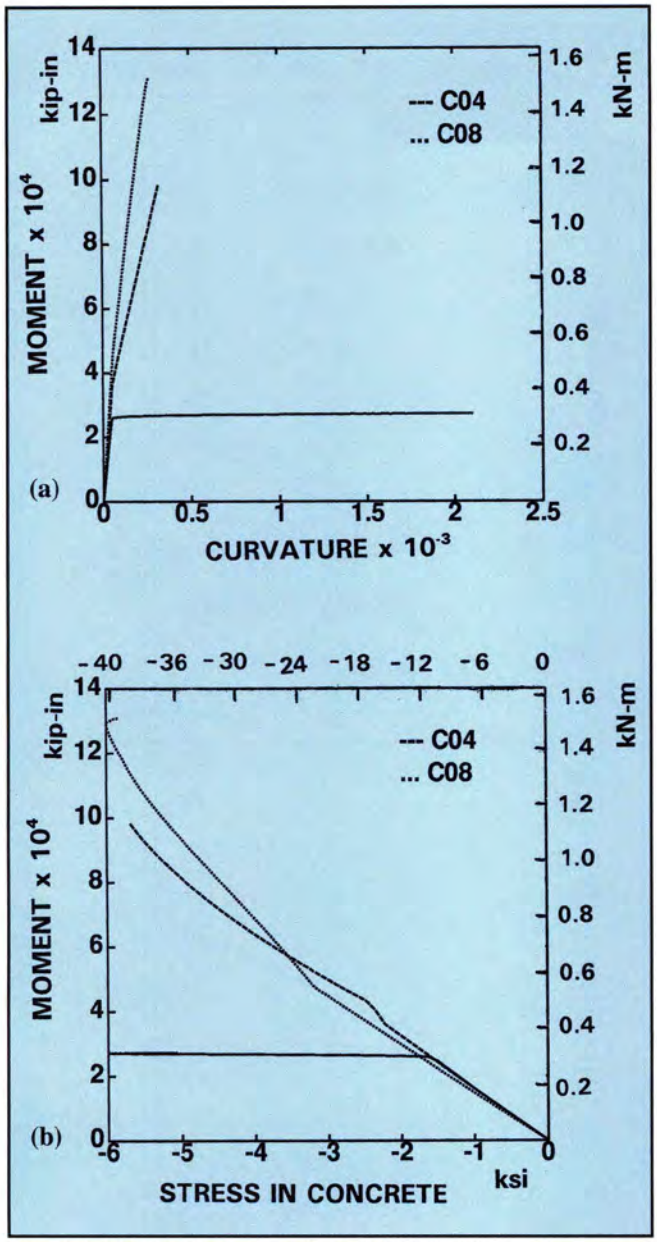

Fig. 7. (a) Moment vs. curvature; (b) Moment vs. stress in concrete.

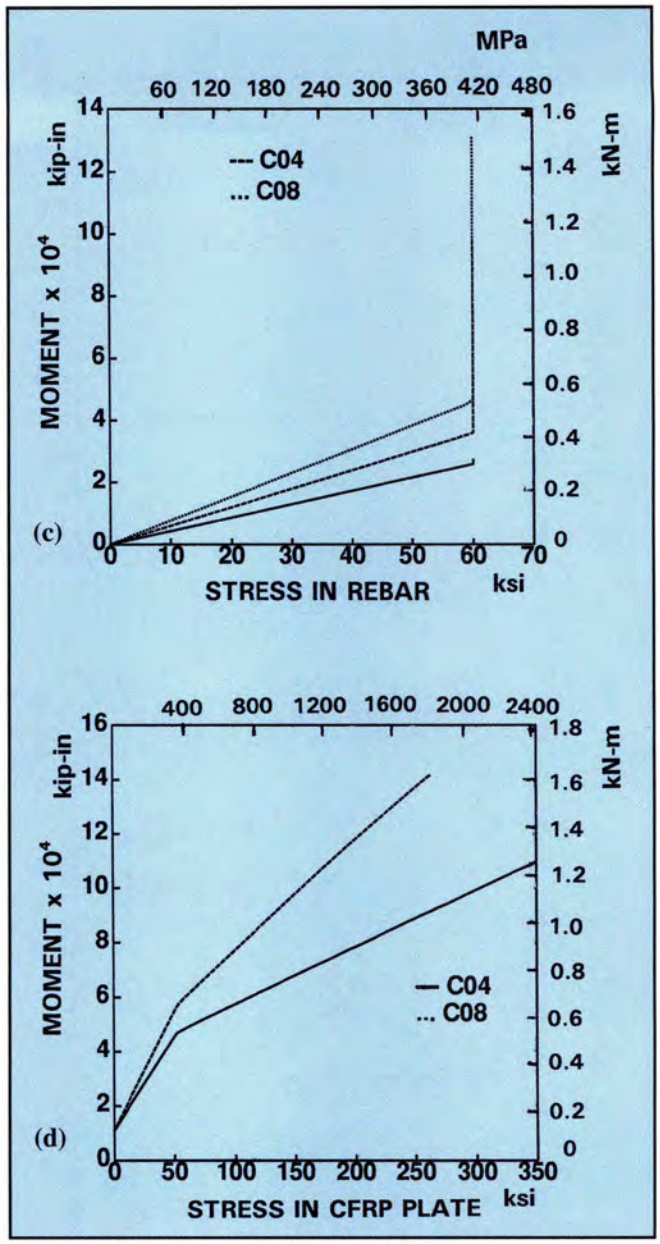

Fig. 7. (c) Moment vs. stress in reinforcing bar; (d) Moment vs. stress in CFRP plate.

bars yield at a higher moment compared to beams strengthened with GFRP plates. The moment vs. stress in the CFRP plate throughout the entire range of loading, up to failure, is shown in Fig. 7(d). For Beam C04, the plate reached its tensile strength at failure of the beam.

Figs. 8(a) through 8(d) show the behavior of the same beam when externally prestressed. The cambering force was the same as that for the beam externally prestressed with GFRP plate; i.e., the initial cambering force eliminated the dead load stresses on top extreme concrete fibers at midspan. The effect of cambering is similar to that observed for the beam cambered with the GFRP plate. The failure capacity in all cases is higher for the beam due to the higher tensile strength of the CFRP plate.

DESIGN EXAMPLE

The following example illustrates how a typical reinforced concrete bridge originally designed for H15 truck loading can be upgraded to HS20 truck loading by bonding composite plates to the tension flange of the girder. The cross section of the girder in the original bridge before strengthening is the same as the T-beam used in the parametric study shown in Fig. 4, but with compression and tension steel areas of 3.09 and 11.04 sq in. (19.93 and 71.22 cm^2), respectively.

The bridge is 60 ft (18.3 m) long and 24 ft (7.3 m) wide, with four girders spaced at 83 in. (2.1 m). The concrete strength is 6000 psi (41 MPa). The dead load, DL1 = 1.84 kips per ft (26.86 kN/m), consists of the weight of the girder and the slab. The superimposed dead load, DL2 = 0.16 kips per ft (2.48 kN/m), consists of the weight of the curbs and wearing surfaces. Fig. 9 shows the curves for maximum moment due to live, dead and superimposed loads. The curves for live load are shown for both H15

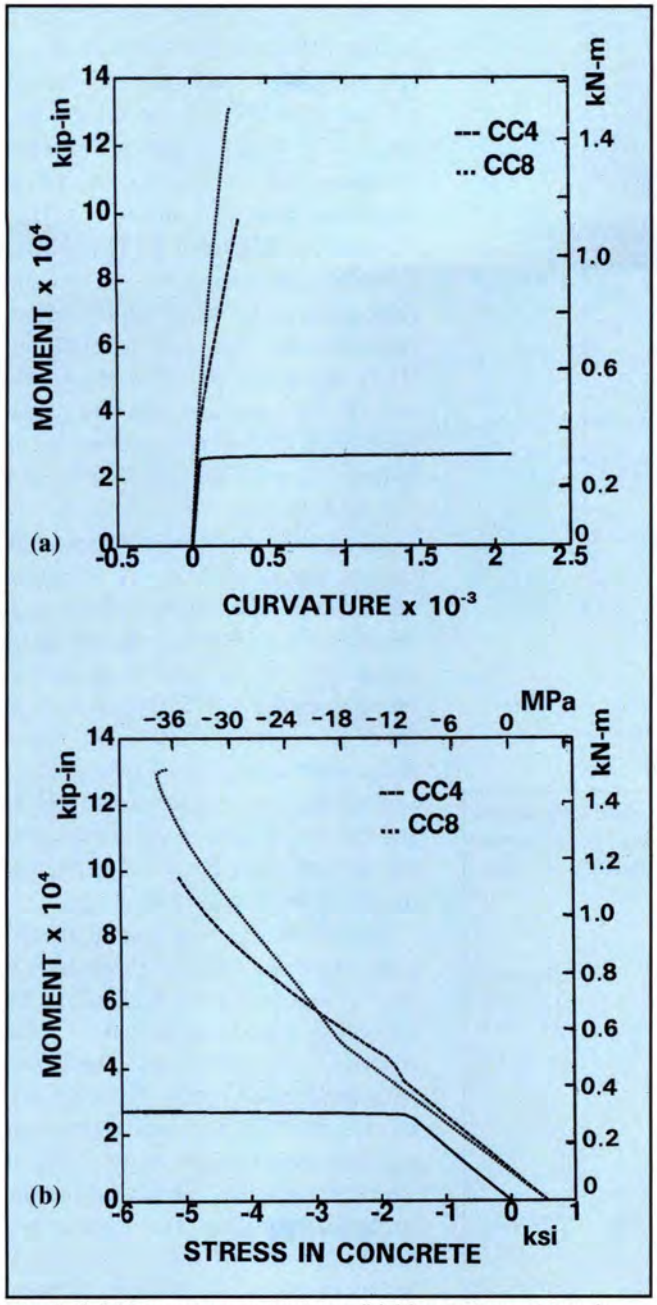

Fig. 8. (a) Moment vs. curvature; (b) Moment vs. stress in concrete.

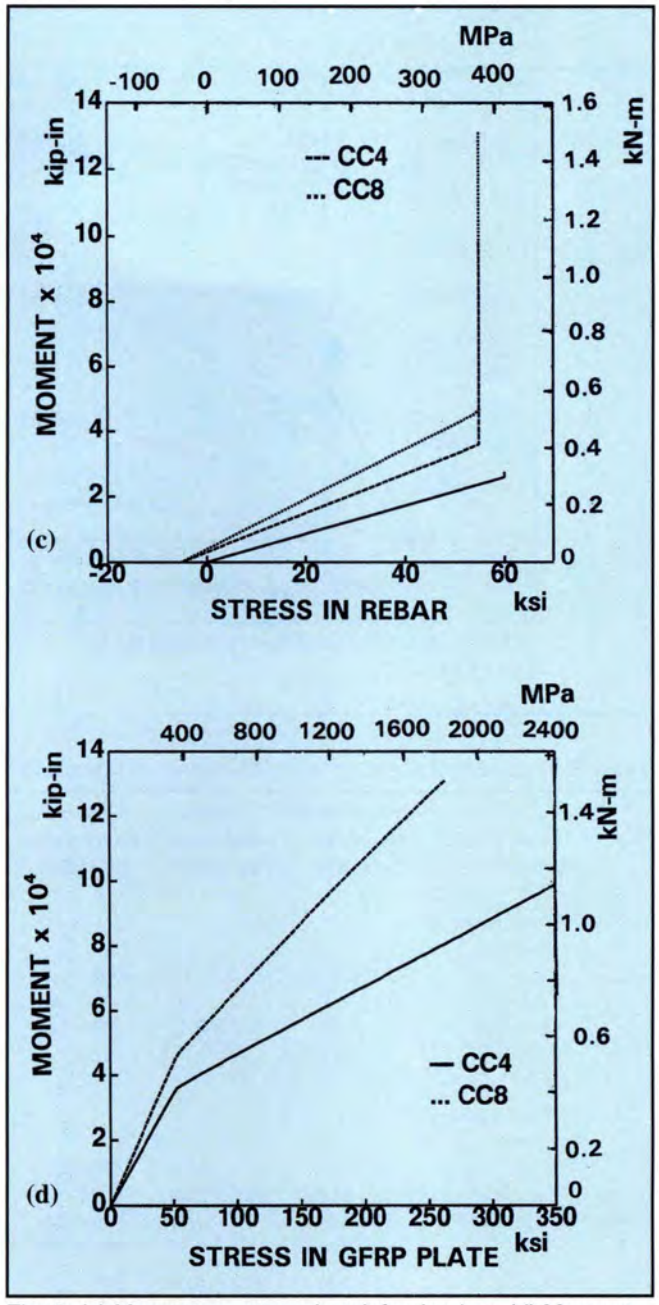

Fig. 8. (c) Moment vs. stress in reinforcing bar; (d) Moment vs. stress in GFRP plate.

Table 2. Summary of stresses and deflections for conventional beams.

Type of loading	Compression steel stress ksi (MPa)	Tension steel stress ksi (MPa)	Concrete flange stress psi (MPa)	Maximum deflection in. (mm)
(a) H15 Truck Loading				
DL1	-3.4 (-23.6)	18.9 (129.8)	-761 (-5.2)	2.61 (66.3)
DL2	-0.3 (-1.9)	1.9 (12.9)	-57 (-0.4)	0.24 (6.1)
LL+1	-0.7 (-4.9)	4.1 (28.3)	-148 (-1.0)	0.39 (9.1)
Total	-4.4 (-30.3)	24.9 (171.0)	-966 (-6.6)	3.24 (81.5)
(b) HS20 Truck Loading				
DL1	-3.4 (-23.6)	18.9 (129.8)	-761 (-5.2)	2.61 (66.3)
DL2	-0.3 (-1.9)	1.9 (12.9)	-57 (-0.4)	0.24 (6.1)
LL+1	-1.4 (-9.4)	9.3 (64.0)	-299 (-2.1)	0.52 (12.8)
Total	-5.1 (-34.9)	30.1 (206.7)	1116 (7.7)	3.37 (85.2)

and HS20 truck loadings.

Four retrofitting alternatives were considered for the bridge:

1. Bonding a GFRP plate, with a cross-sectional area A_{pl} = 2 sq in. (13 cm²), to the tension flange.

2. Cambering the girder with the same plate as in Alternative 1.

3. Bonding a CFRP plate, with a cross-sectional area of A_{pl} = 1 sq in. (6.5 cm²), to the tension flange.

4. Cambering the girder with the same plate as in Alternative 3.

In all cases, cambering is performed by jacking the bridge upward while

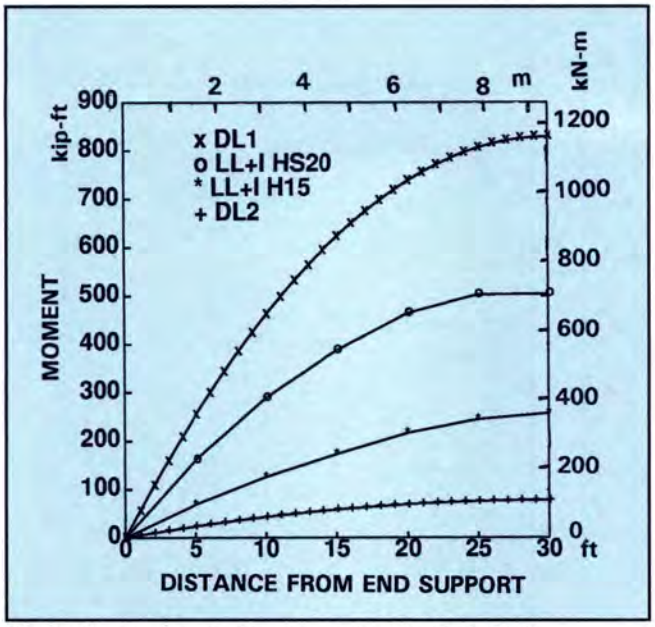

Fig. 9. Curves for maximum moment for DL1, DL2, and LL+1.

Table 3. Summary of stresses and deflections for beam with GFRP plate.

Type of loading	Compression steel stress ksi (MPa)	Tension steel stress ksi (MPa)	Concrete flange stress psi (MPa)	FRP plate stress ksi (MPa)	Maximum deflection in. (mm)
(a) HS20 Truck Loading (no camber)					
DL1	-2.8 (-19.3)	18.0 (123.9)	-609 (-4.2)	0 (0)	2.61 (66.3)
DL2	-0.3 (-2.1)	1.7 (11.7)	-56 (-0.4)	0.5 (3.3)	0.24 (6.1)
LL+1	-1.4 (-9.7)	8.8 (60.5)	-291 (-2.0)	2.5 (17.1)	0.52 (12.8)
Total	-4.5 (-31.1)	28.5 (196.1)	-956 (-6.6)	3.0 (20.4)	3.37 (85.2)
(b) HS20 Truck Loading (camber)					
Prestress	3.3 (22.7)	-5.1 (-35.1)	580 (4.0)	0 (0)	-0.32 (-8.1)
DL1	-2.8 (-19.3)	18.0 (123.9)	-609 (-4.2)	5.07 (34.88)	2.61 (66.3)
DL2	-0.3 (-1.9)	1.7 (11.7)	-56 (-0.4)	0.48 (3.3)	0.24 (6.1)
LL+1	-1.4 (-9.4)	8.8 (60.5)	-291 (-2.0)	2.5 (17.1)	0.52 (12.8)
Total	-1.2 (-7.9)	23.4 (161.0)	-376 (-2.6)	8.0 (55.2)	3.05 (77.2)

Table 4. Summary of stresses and deflections for beam with CFRP plate.

Type of loading	Compression steel stress ksi (MPa)	Tension steel stress ksi (MPa)	Concrete flange stress psi (MPa)	FRP plate stress ksi (MPa)	Maximum deflection in. (mm)
(a) HS20 Truck Loading (no camber)					
DL1	-2.8 (-19.3)	17.5 (120.4)	-612 (-4.2)	0 (0)	2.61 (66.3)
DL2	-0.3 (-2.1)	1.6 (11.0)	-55 (-0.4)	1.42 (9.8)	0.24 (6.1)
LL+1	-1.4 (-9.7)	8.6 (59.2)	-291 (-2.0)	7.4 (51.1)	0.52 (12.8)
Total	-4.5 (-31.1)	27.7 (190.6)	-958 (-6.6)	8.8 (60.9)	3.37 (85.3)
(b) HS20 Truck Loading (camber)					
Prestress	3.3 (22.7)	-5.1 (-35.1)	580 (4.0)	0 (0)	-0.32 (-8.1)
DL1	-2.8 (-19.3)	17.5 (120.4)	-612 (-4.2)	15.2 (104.6)	2.61 (66.3)
DL2	-0.3 (-1.9)	1.6 (11.0)	-55 (-0.4)	1.42 (9.8)	0.24 (6.1)
LL+1	-1.4 (-9.4)	8.6 (59.2)	-291 (-2.0)	7.4 (51.1)	0.52 (12.8)
Total	-1.2 (-7.9)	22.7 (156.1)	-378 (-2.6)	24.0 (165.5)	3.05 (77.2)

in loose contact with epoxy coated composite plates. The jacking forces consist of two concentrated loads of 62 kips (276 kN) separated by a distance of 9 ft (2.74 m) and applied symmetrically about the midspan, resulting in a maximum negative moment of 1572 kip-ft (2131 kN-m).

Table 2 summarizes the stresses and deflections in the bridge girder, before strengthening, for both the H15 and HS20 truck loading. The allowable stresses for steel and concrete calculated from AASHTO equations are as follows: f_s = 24 ksi (165.2 MPa) and f_c = 2400 psi (16.5 MPa).[13]

As can be seen from the table, the stresses due to H15 truck loading are below their allowable values and, therefore, the design of the bridge is satisfactory for the loading. However, the stresses due to HS20 truck loading are in excess of the allowable values and are not acceptable. Tables 3 and 4 summarize the stresses in the girder and the deflections in the girder after the strengthening for the four alternative methods discussed above.

The stresses in beams strengthened with GFRP and CFRP plates but without camber are slightly higher than the allowable stresses as provided in the AASHTO specifications. The externally prestressed beams, however, satisfy the AASHTO allowable stress requirements. The ultimate flexural strength was also calculated for the strengthened girders. The nominal moment capacity of the strengthened beams exceeded the required moment capacity for HS20 loading by 150 percent for both GFRP and CFRP plates. Therefore, the application of composite laminates does provide a feasible solution for strengthening this bridge.

Beams that have been strengthened for flexure may fail in shear. For the example presented here, sufficient shear reinforcement was provided to prevent this failure. In general, though, flexural strengthening may require that the shear strength of the beam be increased as well. This can be achieved by epoxy bonding sheets of composite plates or fabrics to the web of the beam. The behavior of such a system is currently under investigation by University of Arizona researchers at the Federal Highway Administration Laboratories.

CONCLUSION

External prestressing of concrete girders with epoxy-bonded plates significantly increases the allowable and ultimate loads. The strain compatibility method used in the development of the theoretical formulations provides close agreement with experimental results. This method can be used for the design of new structures or for upgrading existing structures.

The successful application of this technique requires careful preparation of the concrete surface and the use of a suitable epoxy. Rubber-toughened epoxies are particularly suitable for this application. The long-term performance of this type of structure, particularly the creep of epoxy in the case of cambered girders and the fatigue for both cambered and uncambered girders, needs to be studied.

REFERENCES

1. Saadatmanesh, H., Albrecht, P., and Ayyub, B. M., "Experimental Study of Prestressed Composite Beams," *Journal of Structural Engineering*, V. 115, No. 9, September 1989, pp. 2348-2363.
2. Saadatmanesh, H., Albrecht, P., and Ayyub, B. M., "Analytical Study of Prestressed Composite Beams," *Journal of Structural Engineering*, V. 115, No. 9, September 1989, pp. 2364-2381.
3. Saadatmanesh, H., Albrecht, P., and Ayyub, B. M., "Guidelines for Flexural Design of Prestressed Composite Beams," *Journal of Structural Engineering*, V. 115, No. 11, November 1989, pp. 2944-2961.
4. MacDonald, M. D., and Calder, A. J. J., "Bonded Steel Plating for Strengthening Concrete Structures," *International Journal of Adhesion and Adhesives* (Guilford), V. 2, No. 2, April 1982, pp. 119-127.
5. Jones, R., Swamy, R. N., Bloxham, J., and Boulderbalah, A., "Composite Behavior of Concrete Beams with Epoxy Bonded External Reinforcement," *International Journal of Cement Composites and Lightweight Concrete* (Harlow), V. 2, No. 2, May 1980, pp. 91-107.
6. Saadatmanesh, H., and Ehsani, M. R., "Fiber Composite Plates Can Strengthen Beams," *Concrete International*, V. 12, No. 3, March 1990, pp. 65-71.
7. Saadatmanesh, H., and Ehsani, M. R., "RC Beams Strengthened with GFRP Plates, I: Experimental Study," *Journal of Structural Engineering*, V. 117, No. 11, November 1991, pp. 3417-3433.
8. Ritchie, P. A., Thomas, D. A., Lu, Le-Wu, and Connelly, G. M., "External Reinforcement of Concrete Beams Using Fiber Reinforced Plastics," *ACI Structural Journal*, V. 88, No. 4, July-August 1991, pp. 490-499.
9. Meier, U., Deuring, M., Meier, H., and Schwegler, G., "Strengthening of Structures with Advanced Composites," in J. L. Clarke (Editor), *Alternative Materials for the Reinforcement and Prestressing of Concrete*, Blackie Academic & Professional, London, 1993, pp. 153-171.
10. Triantafillou, T. C., Deskovic, N., and Deuring, M., "Strengthening of Concrete Structures with Prestressed Fiber Reinforced Plastic Sheets," *ACI Structural Journal*, V. 89, No. 3, May-June 1992, pp. 235-244.
11. Mallick, P. K., *Fiber-Reinforced Composites*, Marcel Dekker, Inc. 1988.
12. Park, R., and Paulay, T., *Reinforced Concrete Structures*, John Wiley & Sons, New York, NY, 1975.
13. AASHTO, *Standard Specifications for Highway Bridges* (1989), American Association of State Highway and Transportation Officials, Washington, D.C.